DOI 10.1007/s00702-006-0434-5
J Neural Transm (2006) 113: 1403–1415

Journal of Neural Transmission
Printed in Austria

Comparison of spatial and temporal pattern for fMRI obtained with BOLD and arterial spin labeling

A. Federspiel[1], **T. J. Müller**[1], **H. Horn**[1], **C. Kiefer**[1,2], and **W. K. Strik**[1]

[1] Department of Psychiatric Neurophysiology, University Hospital of Clinical Psychiatry, Bern, and
[2] Department of Neuroradiology, University of Bern, Switzerland

Received October 5, 2005; accepted January 22, 2006
Published online April 11, 2006;

Summary. Functional magnetic resonance imaging (fMRI) is presently either performed using blood oxygenation level-dependent (BOLD) contrast or using cerebral blood flow (CBF), measured with arterial spin labeling (ASL) technique. The present fMRI study aimed to provide practical hints to favour one method over the other. It involved three different acquisition methods during visual checkerboard stimulation on nine healthy subjects: 1) CBF contrast obtained from ASL, 2) BOLD contrast extracted from ASL and 3) BOLD contrast from Echo planar imaging. Previous findings were replicated; i) no differences between the three measurements were found in the location of the activated region; ii) differences were found in the temporal characteristics of the signals and iii) BOLD has significantly higher sensitivity than ASL perfusion. ASL fMRI was favoured when the investigation demands for perfusion and task related signal changes. BOLD fMRI is more suitable in conjunction with fast event related design.

Keywords: fMRI, CBF, BOLD, arterial spin labeling, impulse response, primary visual cortex.

Introduction

Functional magnetic resonance imaging (fMRI) is used to visualize regional brain activity non-invasively. Two methods are employed in fMRI: one based on blood oxygenation level dependent (BOLD) contrast, being sensitive to changes in blood oxygenation, and one based on arterial spin labeling (ASL) perfusion contrast, manifested as cerebral blood flow (CBF) is a valuable research tool for mapping brain activity. The spatial resolution of BOLD fMRI depends strongly on the strength of the magnetic filed (Chen et al., 1999) and varies between few 100 µm (i.e. the size of dominance columns in the primary visual cortex) and few millimeters. The BOLD signal is the complex result of interactions between CBF, cerebral blood volume (CBV) and cerebral metabolic rate of oxygen (CMRO2) (Kwong et al., 1992; Ogawa et al., 1993) and is detected as change in $T2^*$ (i.e. local magnetic field distortion). Due to regional brain activation an increase in $T2^*$ can be observed. fMRI based on BOLD contrast therefore measures neuronal activity indirectly via its assumed haemodynamic correlate. The interpretation of the

BOLD signal depends on the nature of the underlying neural activity that evokes the haemodynamic response. Furthermore, BOLD contrast is originated by intravascular deoxyhemoglobin changes and it was suggested, that the BOLD signal is mainly an effect produced by macroscopic veins (Lai et al., 1993). Typical applications of BOLD fMRI concentrate on the basic exploration of sensory modalities, motor functions, somatosensory processing and the cortical topography of cognition [see Di Salle et al. (1999) for a detail review].

The temporal response of the BOLD signal in the primary visual cortex was measured (Boynton et al., 1996) and its dynamic properties could be modeled. This model comprises instantaneous nonlinearity that transforms image contrast to neural response, followed by a linear temporal filter. The exact relation between the underlying neural activity and the resulting physiological responses in CBF, cerebral metabolic rate of oxygen (CMRO2) and cerebral blood volume (CBV) is still not fully understood. Nonetheless, models that explain the shape of the BOLD response were developed (Buxton et al., 1998; Mandeville et al., 1999) that account for the post-stimulus undershoot of the BOLD response.

In summary, BOLD fMRI offers a method for mapping brain activity and for extracting response functions. However, because of its complex relation to the mentioned physiological quantities, it remains a method that has distinct limitations as to the interpretation of the underlying neural activity.

Arterial spin labeling (ASL) techniques were first proposed by Detre et al. (1992). The experiments have later been extended to humans by Roberts et al. (1994). Tagged arterial water protons that are used as tracer have a non-equilibrium longitudinal magnetization that is smaller than the equilibrium longitudinal magnetization of fully-relaxed brain water protons. The reduction of the MR signal intensity due to the inflow of labeled arterial water into the imaging slice can be interpreted using the classical tracer kinetic theory to obtain a quantitative image of cerebral blood flow. The ASL techniques are traditionally divided into continuous arterial spin labeling (CASL, see Detre et al. (1992)) where a steady state reduction of magnetization is obtained in a thin slice, and pulsed arterial spin labeling (PASL) using short radiofrequency labeling pulses to tag a thick slab prior to the imaging slice (Calamante et al., 1999). The short decay time of the tracer (approximately 1 s) prevents a significant tracer accumulation in venous structures. Therefore, the signal changes in perfusion fMRI are not observed over veins and the localization of signal changes is constricted over activated cortex (Silva et al., 1999). One of the major limitations of ASL fMRI techniques is the restricted brain coverage. Only recently whole-brain ASL fMRI was assessed using CASL (Talagala et al., 2004; Garraux et al., 2005).

Recently ASL perfusion contrast was investigated in healthy controls during visual stimulation experiments (Zhu et al., 1998; Yang et al., 2004), finger tapping task (Wang et al., 2003b) and overt speech production (Kemeny et al., 2004). The clinical use of perfusion based fMRI extends over a broad choice of clinical settings including acute stroke, chronic cerebrovascular disease, degenerative diseases and epilepsy [see Detre et al. (1999) for a detailed review]. In patients with Alzheimer's dementia it was demonstrated that flow decreases relative to control subjects in temporal, parietal, frontal, and posterior cingulate cortices (Alsop et al., 2000). In pediatric field, differences between absolute CBF values of neurologically normal children as compared to adult was observed (Wang et al., 2003c). Based on selected children with neurologic diseases, the same group could also demonstrate the feasibility in the diagnosis of pediatric brain disorders (Wang et al., 2003c).

In summary, both methods (BOLD contrast and arterial spin labeling perfusion contrast) are currently employed for fMRI experiments. Which of the two are the best? Is there any advantage in preferring one method to the other? The present study was conducted to reproduce previous findings and to provide practical hints when planning fMRI experiments. Therefore, this paper compares the spatial and temporal characteristics of BOLD and arterial spin labeling perfusion fMRI.

Material and methods

Participants

Nine volunteers (4 females and 5 males) participated in the study. Mean ($\pm$SD) age was 29.7 ± 4.6 years. All subjects were right-handed, as assessed by the Edinburgh Inventory (Oldfield, 1971). Vision was normal or corrected-to-normal in all subjects, and none had a history of major medical, neurological or psychiatric diseases. The investigation was conducted in accordance with the Declaration of Helsinki and approved by the local ethical committee. All subjects gave written informed consent to participate in the study prior to the investigation.

Experimental paradigm

The stimulus consisted in 1 Hz full-field black and white alternating checkerboard visual stimulation. A red fixation cross was constantly visible. Stimuli were presented to the subjects by a goggle system (VisuaStim XGA, Resonance Technology, Inc. USA). The parameters of this system were: field of view $= 30°$, refresh rate $= 60$ Hz, resolution $= 1024 \times 768$. Subjects were asked to gaze a fixation cross. Two different experiments were conducted: experiment #1 for the ASL perfusion contrast measurements with cycle of 30 seconds (s) ON and 30 s OFF, repeated 12 times resulting in a total presentation time of 720 s; experiment #2 for the fMRI-BOLD contrast measurements with cycle of 15 s ON and 15 s OFF, repeated 12 times resulting in a total presentation time of 360 s. The temporal parameters in both experiments were chosen to allow direct comparison of the investigated methods. Therefore, the two stimulus categories are labeled by ''Resting'' for the OFF cycles and ''Visual stimulation'' for the ON cycles respectively.

MRI acquisition

All images were acquired using a 1.5 T whole body MRI system (Siemens Vision, Erlangen, Germany), equipped with a standard radio frequency head coil. The fMRI session included the acquisition of a set of 3D T1-weighted (Magnetization Prepared Rapid Acquisition Gradient Echo, MP-RAGE) images, providing 192 sagittal slices with 1.0 mm thickness, 256 mm $\times$ 256 mm field of view (FOV) and a matrix size of 256×256. Further scan parameters were: 11.4 ms repetition time (TR), 4.4 ms echo time (TE) and a flip angle of 15° (FA).

fMRI acquisition

Functional images were acquired using a multi-slice single-shot $T2^*$-weighted echo planar imaging sequence, with 20 interleaved axial oblique slices, positioned in-line with the bi-commissural axis. 144 dynamic scans were collected in each subject (TR $= 2500$ ms, TE $= 60$ ms, FA $= 90°$, slice thickness $= 4$ mm, gap thickness $= 0$ mm, matrix size $= 64 \times 64$, FOV $= 230$ mm $\times$ 230 mm). The sequence has been driven in 3D PACE mode (Siemens Erlangen) enabling prospective motion correction.

ASL acquisition

The labeling method used in this work is applied as pulsed arterial spin labeling (PASL) and has been described elsewhere (Wong et al., 1997, 1998, 1999; Luh et al., 1999) and is referred to as QUIPPS II with thin-slice TI1 periodic saturation. Arterial spins are labeled by a thick (10 cm) inversion slab, placed proximal to the imaged slices (PICORE labeling scheme) (Luh et al., 1999). During the inversion time TI2, the labeled blood perfuses the tissue in the imaging slices, causing a slight decrease of the MR signal of the tissue. Subtraction of the labeled image from a referring control image assesses this change in signal. The repeated saturation pulses between TI1 and TI1-stop define the time width of the bolus. In the control measurement, the pulse is executed off-resonance.

The PASL parameters are as follows: the gap between the labeling slab and the proximal slice is 10 mm, TI1 $= 700$ ms, TI1 stop time $= 1300$ ms, TI2 $= 1400$ ms, crusher bipolar gradients are switched between slice excitation and readout to reduce signal from large vessels. Further parameters are: repetition time TR $= 2500$ ms, number of measurements N $= 288$, measurement time Tacq $= 12$ min 07 s, TE $= 15$ ms, six slices at a distance of 1.5 mm, slice thickness $= 6.0$ mm, matrix size $= 64 \times 64$, FOV $= 224$ mm $\times$ 224 mm, partial Fourier 6/8, BW $= 3004$ Hz/Px, echo spacing 0.4 ms. The sequence has been driven in 3D PACE

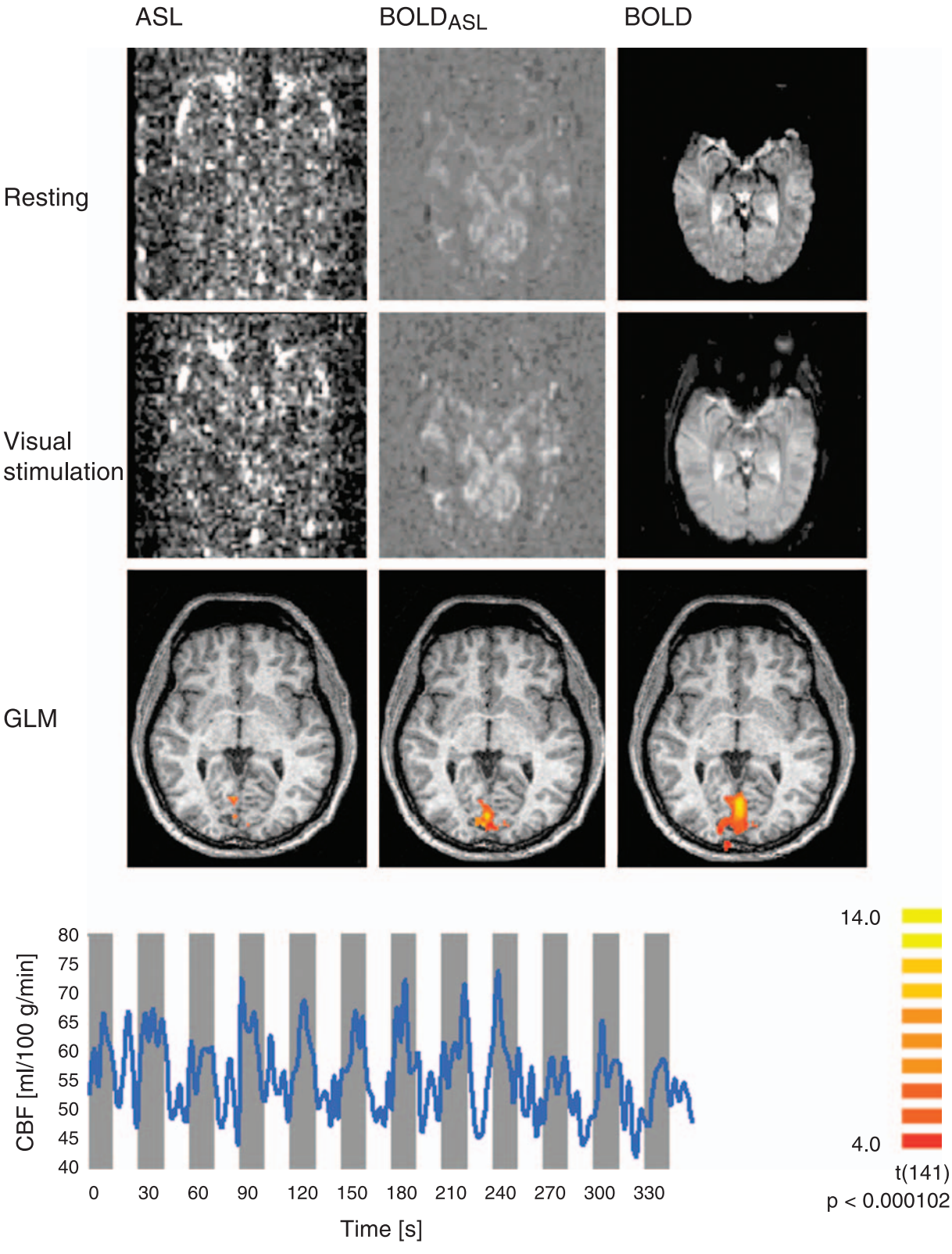
ASL
BOLDASL
BOLD
Resting
Visual stimulation
GLM
CBF [ml/100 g/min]
80
75
70
65
60
55
50
45
40
0
30
60
90
120
150
180
210
240
270
300
330
Time [s]
14.0
4.0
t(141)
p < 0.000102

mode (Siemens Erlangen) to enable prospective motion correction.

fMRI analysis

Analysis of the fMRI data was performed using BrainVoyager QX 1.2 [Brain Innovation, Maastricht, Netherlands, www.BrainVoyager.com]. Preprocessing of the images included the removal of low-frequency drifts, 3-D motion detection and correction and spatial smoothing with 4 mm FWHM. Coregistration of the 2-D functional to the 3-D structural images was performed using the scanner's slice position parameters of the T2*-weighted measurements and the T1-weighted anatomical measurements. The spatial resolution of functional data set was interpolated to isovoxel 1 mm^3. Finally, the anatomical and functional data sets were transformed into the Talairach space (Talairach et al., 1988). Activated voxels in the primary visual cortex were identified using Student t-test between time series and boxcar model function (threshold: $t > 4.0$, $p < 0.0001$). These voxels are referred to as Region of Interest (ROI). The reconstruction of the hemodynamic response function within the ROI was performed using a general linear model (GLM) to estimate the finite impulse response (FIR) associated with the stimulus period (same procedure as described in Lehmann et al. (2004)).

ASL analysis

Analysis of the ASL data was performed using own written MATLAB programs (MATLAB version 6, release 13; The MathWorks, Inc., USA) and with BrainVoyager QX 1.2. As the measured voxel dimension lies in the same range like the spatial smoothing kernel, we decided to apply no temporal and spatial manipulation (''filtering'' or ''smoothing'') of the raw data (Wang et al., 2005). Data of each subject was used to calculate a flow time series (control – labeling) (labeled as condition CBF hereafter) and a BOLD time series by taking the average of the time-matched label and control images (labeled as condition $BOLD_{ASL}$ hereafter) using the same calculation procedure as described elsewhere (Miller et al., 2001; Wang et al., 2003b; Obata et al., 2004). Although the TE is short and not optimized for $BOLD_{ASL}$ contrast, this contrast was additionally used in several other studies for the comparison between CBF and BOLD time series (Aguirre et al., 2002; Miller et al., 2001; Wang et al., 2003a, b, 2005; Yang et al., 2000). It provides an additional measure within the same setup. The difference signal (control – labeling) is proportional to CBF (Luh et al., 1999). The quantification of CBF of the flow time series was performed using the following relation:

$$CBF = \frac{\Delta M}{2M_0 \mathrm{TI1}} e^{\frac{\mathrm{TI2}}{\mathrm{TIb}}}$$

where ΔM is the difference signal (control – labeling); M_0 is the equilibrium brain tissue magnetization; the time constants TI1, TI2 are described above and $\mathrm{TIb} = 1200$ ms is the decay time for labeled blood at 1.5 T.

Activated voxels in the primary visual cortex (ROI) were identified using Student t-test between CBF time series and boxcar model function (threshold: $t > 4.0$, $p < 0.0001$). These ROI were used also for the $BOLD_{ASL}$ analysis. The reconstruction of the CBF and the $BOLD_{ASL}$ response function within the ROI was performed using the same procedure as used for the reconstruction of the hemodynamic response function (i.e. general linear model (GLM) to estimate the finite impulse response (FIR) associated with the stimulus period).

In Fig. 1 the three different acquisition methods are presented with raw images and the GLM analysis for a representative subject (S8), including the CBF time course for the activated brain area.

Results

Analysis of Variance (ANOVA) revealed no significant condition effect for the displacements in x direction ($F_{(2,26)} = 0.014$; n.s.), y direction ($F_{(2,26)} = 1.533$; n.s.) and z direction ($F_{(2,26)} = 0.197$; n.s.) for the center of gravity of the the activated area in early visual cortex. The Talairach coordinate for center of gravity for each subjects are summarized in Table 1. The total number of activated voxels in the primary visual cortex was 9991 for CBF condition, 42476 for $BOLD_{ASL}$ condition and 52663 for BOLD condition and is summarized in Table 1.

Fig. 1. Comparison of the three different acquisition methods: raw images for resting and visual stimulation for a representative subject (S8). Each of the axial image is located at $z = 0$. The contrast between resting and visual stimulation (GLM) is shown in color and the colorbar indicates the t-test values. Also shown is the CBF time course for the activated region in early visual cortex

Table 1. Summary of identified brain regions with Talairach coordinate for center of gravity for resting and visual stimulation for each subject. Separate values of perfusion (mean ± standard deviation), BOLD amplitude extracted from ASL signal and BOLD signal are listed. Additionally, the fitted parameters time to onset and time to peak are listed

Subject	Measure	#Voxel	Talairach coordinates for center of gravity (mean ± SD)			Values for CBF in [ml/100 g/min] BOLD/$BOLD_{ASL}$ [arbitrary]		Time to onset [sec]	Time to peak [sec]
			X [mm]	Y [mm]	Z [mm]	Activation	Resting		
S1	CBF	953	2.1 ± 3.5	−65.8 ± 2.1	−4.7 ± 4.1	62.3 ± 5.2	50.7 ± 5.3	2.59	3.92
	$BOLD_{ASL}$	4870	1.1 ± 4.2	−74.9 ± 7.1	−0.8 ± 5.7	686.3 ± 0.8	683.5 ± 0.5	2.91	3.24
	BOLD	5917	−0.4 ± 5.2	−75.1 ± 7.4	−0.6 ± 5.4	452.2 ± 4.3	450.4 ± 4.7	2.11	4.77
S2	CBF	1009	−5.2 ± 4.6	−83.0 ± 3.6	−7.1 ± 4.8	60.4 ± 4.1	55.4 ± 2.0	2.55	3.74
	$BOLD_{ASL}$	3885	−9.9 ± 4.2	−81.3 ± 6.3	1.9 ± 6.6	637.4 ± 0.7	636.4 ± 1.1	2.54	4.04
	BOLD	2953	−4.4 ± 4.5	−82.1 ± 5.7	−9.4 ± 6.8	358.1 ± 2.1	357.6 ± 2.4	2.08	4.75
S3	CBF	1448	3.3 ± 3.2	−66.4 ± 2.6	−12.4 ± 4.7	62.4 ± 5.7	50.1 ± 3.3	2.12	3.57
	$BOLD_{ASL}$	4642	2.5 ± 4.1	−74.4 ± 7.4	−11.6 ± 5.1	684.3 ± 0.9	681.6 ± 0.5	2.79	3.75
	BOLD	5933	1.3 ± 4.7	−74.2 ± 7.4	−11.8 ± 5.0	413.5 ± 2.4	412.0 ± 2.8	2.35	4.81
S4	CBF	1706	3.3 ± 5.9	−84.2 ± 5.7	−6.6 ± 2.9	110.3 ± 5.5	102.0 ± 3.7	2.77	3.72
	$BOLD_{ASL}$	7958	1.8 ± 6.9	−85.1 ± 6.4	1.6 ± 5.9	547.4 ± 0.7	546.8 ± 0.7	2.86	3.56
	BOLD	11640	0.2 ± 6.9	−86.6 ± 6.5	0.9 ± 6.8	382.1 ± 2.3	381.0 ± 2.2	2.67	5.22
S5	CBF	813	−11.4 ± 1.3	−84.2 ± 4.7	−8.5 ± 3.4	80.4 ± 6.4	68.2 ± 3.4	2.45	3.68
	$BOLD_{ASL}$	10056	−0.1 ± 7.4	−86.1 ± 6.5	−2.3 ± 7.2	578.8 ± 0.6	575.2 ± 0.9	2.88	3.52
	BOLD	11851	−0.7 ± 7.3	−86.9 ± 6.6	−1.9 ± 7.2	374.3 ± 2.2	373.4 ± 2.1	2.71	4.85
S6	CBF	1081	0.7 ± 3.1	−74.6 ± 4.2	0.9 ± 2.6	60.5 ± 5.4	55.2 ± 2.7	2.56	3.55
	$BOLD_{ASL}$	1737	−0.2 ± 3.6	−79.3 ± 7.6	1.2 ± 3.1	620.1 ± 1.2	615.8 ± 0.9	2.74	3.48
	BOLD	2061	−0.3 ± 3.4	−80.1 ± 7.4	0.7 ± 3.4	433.2 ± 4.2	432.5 ± 3.9	2.75	4.82
S7	CBF	59	6.6 ± 1.6	−78.1 ± 1.3	−7.6 ± 0.9	57.2 ± 3.9	49.0 ± 5.4	2.19	3.61
	$BOLD_{ASL}$	2641	3.6 ± 5.1	−83.8 ± 4.5	−16.3 ± 4.9	312.6 ± 0.8	311.1 ± 0.7	2.55	3.89
	BOLD	3545	3.7 ± 4.8	−84.1 ± 4.5	−15.3 ± 5.0	234.2 ± 0.4	232.8 ± 1.2	2.67	5.09
S8	CBF	2219	5.0 ± 5.8	−75.5 ± 5.6	3.0 ± 4.1	60.0 ± 3.0	52.2 ± 1.9	2.49	3.58
	$BOLD_{ASL}$	4391	3.7 ± 5.3	−77.9 ± 7.3	4.2 ± 4.5	679.6 ± 0.4	677.0 ± 0.4	2.77	3.81
	BOLD	5527	2.3 ± 5.7	−78 ± 7.1	3.2 ± 4.6	451.7 ± 3.0	450.2 ± 2.8	2.58	5.18
S9	CBF	703	−2.6 ± 2.3	−74.8 ± 4.1	−5.4 ± 2.9	78.4 ± 4.3	72.9 ± 6.6	2.58	3.81
	$BOLD_{ASL}$	2296	−2.5 ± 2.2	−79.7 ± 5.1	−9.8 ± 11.7	502.2 ± 1.3	498.9 ± 1.3	2.88	3.93
	BOLD	3236	−3 ± 2.5	−74.6 ± 4.1	−5.1 ± 3.1	454.7 ± 6.0	454.7 ± 6.0	2.61	4.99

ANOVA revealed significant differences in the number of voxel between the three conditions ($F_{(2,26)} = 7.953$; $p < 0.002$). Post-hoc multiple comparison of mean voxel values according to Scheffé revealed significant differences between CBF and $BOLD_{ASL}$ (mean difference (MD): −3609.4444; Confidence Limit (CL): [−6848.8; −370.0]; $p < 0.027$) and between CBF and BOLD group (MD: −4741.3; CL: [−7980.7; −1501.9]; $p < 0.003$). For each subject the regions of interest that surpassed the threshold condition are presented on Fig. 2 for $BOLD_{ASL}$- and CBF-condition. The regions of interest for each subject for BOLD and CBF are shown on Fig. 3. The average time curves for CBF, $BOLD_{ASL}$ and BOLD are shown in Fig. 4. We found significant correlation coefficient for the time course between BOLD and CBF ($r = 0.7466$; $p < 0.0053$); between $BOLD_{ASL}$ and CBF ($r = 0.8413$; $p < 0.0006$) and between $BOLD_{ASL}$ and BOLD ($r = 0.9049$; $p < 0.0001$).

A gamma variate function was fit to the time series of all three measurement to model the hemodynamic response yielding as parameter: i) time to onset of the hemodynamic response and ii) the time to peak of activation (Miller et al., 2001). These parameters are summarized in Table 1. In the ANOVA, the time to onset parameter revealed significant differences in the three conditions $F_{(2,26)} = 5.57$, $p < 0.01$. The Post-hoc t-tests revealed significant differences between BOLD and $BOLD_{ASL}$ $t_{(16)} = 2.62$, $p < 0.018$, and significant differences between $BOLD_{ASL}$ and CBF $t_{(16)} = 3.64$, $p < 0.002$. The mean (±SD) values were: BOLD: 2.50 ± 0.26; $BOLD_{ASL}$: 2.77 ± 0.14; CBF: 2.48 ± 0.20. In the ANOVA, the time to peak parameter revealed significant differences in the three conditions $F_{(2, 26)} = 142.16$, $p < 0.0001$. The Post-hoc t-tests revealed significant differences between BOLD and $BOLD_{ASL}$ $t_{(16)} = 9.66$, $p < 0.0001$, and significant differences between BOLD and CBF $t_{(16)} = 7.25$, $p < 0.0001$. The mean (±SD) values were: BOLD: 4.94 ± 0.18; $BOLD_{ASL}$: 3.61 ± 0.16; CBF: 3.77 ± 0.20.

The qualitative result for the CBF signal is that the flow experiences an overshoot at the beginning and end of the stimulus. An overshoot at the beginning and end of the stimulus was also qualitatively found for the BOLD response.

Discussion

Here we could demonstrate that all functional methods applied in this study (i.e. CBF, BOLD and $BOLD_{ASL}$) were able to reflect neural activity evoked by visual stimulation. No differences between the three measurements were found in the location of the activated region, as there were no statistical differences in Talairach coordinate for the center of gravity. No differences between the three measurements were found for the temporal shape of the signals; we observed significant correlations between the three time curves. However, the time to onset and time to peak parameters differs between the three measurements. The visual stimulus evoked activated volume that was found to be similar for the BOLD and $BOLD_{ASL}$ measures, but substantial reduced for the CBF measurement as obtained by ASL. The properties of BOLD and ASL perfusion fMRI are listed side-by-side in Table 2.

Visual stimulation with checkerboard paradigm evokes a distinct cortical response pattern located in early visual areas. This has been shown in a number of fMRI studies with BOLD contrast (Hansen et al., 2004; DeYoe et al., 1994; Blamire et al., 1992) and with perfusion contrast by means of ASL (Yang et al., 2000, 2004; Gonzalez-At et al., 2000).

All three methods localize the activated brain region in the same center of gravity, as expressed in terms of Talairach coordinates, although the nature of BOLD contrast is attributed to an effect produced by macroscopic veins (Lai et al., 1993), whereas the

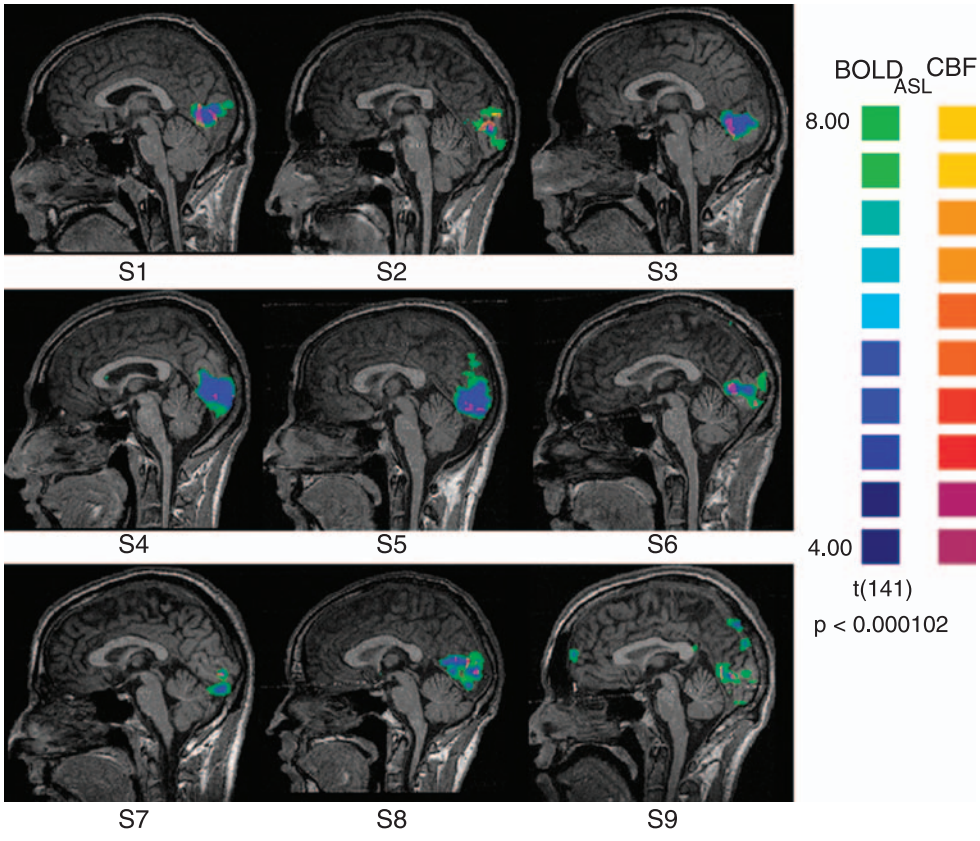
BOLD
ASL
CBF
8.00
4.00
t(141)
p < 0.000102
S1
S2
S3
S4
S5
S6
S7
S8
S9

Fig. 2

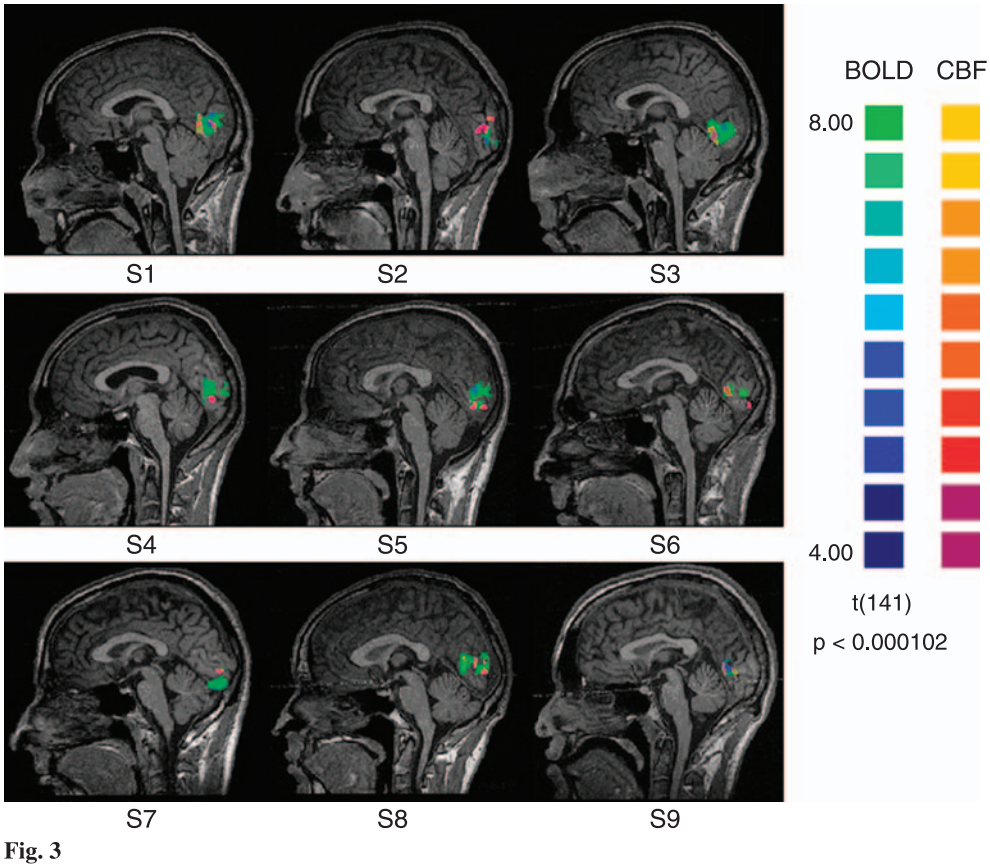
BOLD
CBF
8.00
4.00
t(141)
p < 0.000102
S1
S2
S3
S4
S5
S6
S7
S8
S9

Fig. 3

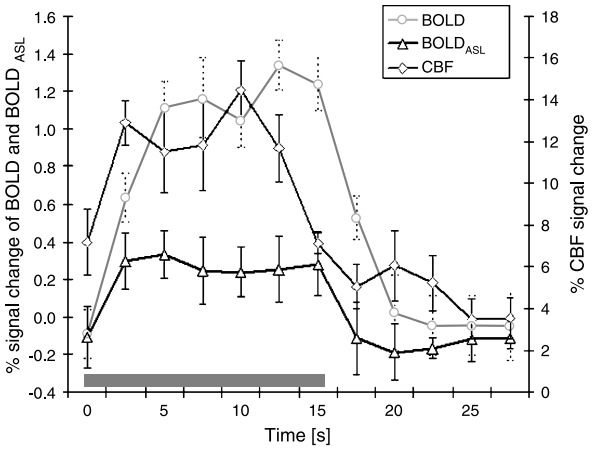

Fig. 4. Signal time course in early visual areas obtained as contrast between resting and visual stimulation. BOLD signal in light grey and BOLD extracted from ASL measurement in black. The % signal change of these modalities is on the right. The time course for ASL perfusion is shown in grey with different scale located on the left

signal changes in perfusion contrast are not observed in veins but in the capillary bed (Silva et al., 1999; Detre et al., 2002).

We observed significant differences in the amount of the activated area in the visual cortex between CBF and BOLD and between CBF and $BOLD_{ASL}$. The total volume detected by CBF was significant lower as compared to the volume detected by BOLD and $BOLD_{ASL}$. A recent PET and fMRI study (Feng et al., 2004) did not report these differences in activated volume. The discrepancy between these results and our findings may originate by the threshold of t-test value used in our study. In fact, we used the same t-test value as threshold in all three methods and the contrast was testing the same effect over subjects (resting vs. visual activation). By doing so, we were evaluating the sensitivity of the three methods in detecting activated voxels, keeping the false-positive rate (FPR) for the three methods at same value. In all subjects, the suprathreshold voxels detected within the visual cortex for CBF perfusion contrast were a subset of those voxels discovered by BOLD and $BOLD_{ASL}$, a finding that is consistent with a combined BOLD and perfusion fMRI study that found a smaller total activated area for CBF perfusion as compared to BOLD fMRI (Aguirre et al., 2002). The number of voxels within the acti-

Table 2. Synopsis of the properties of the different acquisition modalities BOLD and ASL

Property	BOLD-fMRI	ASL-fMRI
Sensitivity	High	Low
Quality of measure	Relative	Absolute
Hemodynamic signal extraction?	Yes	Yes
Measured physiological signal	Composed (CBF, CBV, $CMRO_2$)	Unique (CBF)
Spatial specificity	Venules and draining veines	Capillaries, arterioles
Repetition time	>1 sec	>2 sec
Position parametes	Variable	Fixed
Imaging volume	Whole brain	Part of brain (PASL) Whole brain (CASL)

Fig. 2. Sagittal images of each subject with the contrast between resting and visual stimulation. The colorbar indicates the t-test values and red/yellow colors represents results for the ASL measurement; blue/green colors represents results for the BOLD measurement

Fig. 3. Sagittal images of each subject with the contrast between resting and visual stimulation. The colorbar indicates the t-test values and red/yellow colors represents results for the ASL measurement; blue/green colors represents results for the BOLD signal extracted from ASL measurement

vated area in the visual cortex showed large variability between the subjects. This reflects other studies showing that the visual cortex differs inter-individually in size and in location (Dougherty et al., 2003; Hasnain et al., 1998; Rombouts et al., 1998).

The observed ASL perfusion amplitude in the early visual areas agree with previous MR study (Kwong et al., 1992) and with PET Studies (Fox et al., 1984, 1985).

The time to onset and time to peak parameters were significantly different in the three measurements. These differences in temporal parameters could be originated by signal from different voxels. In fact, the activated region measured by ASL is smaller than the activated region measured by BOLD. The observed hemodynamic responses in the smaller brain region and in the larger brain region are different. These differences in hemodynamic response were also found in primary motor areas and supplementary motor areas using a finger-tapping task (Obata et al., 2004). The authors used two different ''balloon model'' calculations (Buxton et al., 2004) to theoretically describe the descripancies between the temporal responses of CBF and BOLD signal in both brain areas. A variation of the time to onset across voxel was also found in animal studies (Silva et al., 2000). Nonetheless, the shape of the time course of the ASL perfusion correlates with the time courses of both BOLD contrast measurements (BOLD and $BOLD_{ASL}$) suggesting that not the whole time course is different, but only distinct time points.

Additionally, we observed that the CBF- and the BOLD signal experienced an overshoot at the beginning and end of the stimulus. This time pattern was also found in the supplementary motor area but not in the primary motor area during the finger-tapping experiment (Obata et al., 2004). An overshoot of BOLD and CBF values in primary visual area V1 was also demonstrated in a combined BOLD and CBF sudy using checker-board stimulation (Hoge et al., 1999). The authors measured CBF with a flow-sensitive alternating inversion recovery (FAIR) seqeuence; hence, a direct comparison of this finding with ASL perfusion data is limited.

In summary we observed that during visual stimulation the early visual area was activated as measured with three different methods sensitive to perfusion contrast and to BOLD contrast. The localization power of the three methods was very similar and the coordinates of the centers of gravity of the regions of interest did not differ significantly. The temporal characteristics of the signals were also found to be similar. It is therefore not possible to favor one method over the other given these parameters of this study.

However, since ASL perfusion requires longer repletion time as compared to BOLD fMRI studies, it is reasonable to propose ASL contrast for experiments with block-design. In contrary, BOLD fMRI experiments allows rapid event-related design, which is more adequate to resolve the physiological parameters associated to neural activity, connected to fast single stimuli. Furthermore, the sensitivity to detect significant brain activations of BOLD fMRI was higher compared to ASL. BOLD fMRI offers further advantages over ASL fMRI when considering the freedom in selecting the acquisition parameters. In fact, BOLD fMRI allows a wide range of settings like TR, TE, slice positioning and slice thickness. These settings cannot be modified in ASL experiments. These considerations would favor BOLD fMRI over ASL fMRI. BOLD fMRI on the other hand is an observable that is composed of an uncertain combination of basic quantities like CBF, CBV, CMRO2; and the relation of these quantities with neural activity is still not fully understood.

On the other hand, ASL fMRI provides a direct measure of one specific quantity; i.e. CBF. ASL fMRI measurement offers reliable

absolute perfusion values in the brain tissue during resting as well as during task performances. This offers the possibilities to compare single values among different subjects. With BOLD fMRI it is only possible to compare the percentual signal changes among different subjects; it provides only information on the additional amount a stimulus produces over a baseline. The advantage of ASL can be applied in studies comparing mental and neurological diseases to other pathologies or to normal population. In these populations the basic metabolism can be altered, that may also influence the BOLD signal.

Beside the perfusion quantity obtained with ASL fMRI, it is additionally possible to extract BOLD images within the same session. This is a clear advantage over pure BOLD fMRI experiments.

In conclusion, ASL fMRI is at present a valuable choice when planning investigations with block design. This allows besides the pure extraction of signal changes between resting- and task condition, the obtaining of absolute perfusion values. BOLD fMRI is the right choice when fast event-related experiments focus on brain processing of complex tasks. If future improvements of ASL fMRI technique will allow the amply modification of the setting parameters (like shorter acquisition time), the question of choosing the right acquisition method will further weighting the ASL method.

Acknowledgments

This research was supported by the Schweizerische Nationalfond SNF grant (3200B0-100823).

References

Aguirre GK, Detre JA, Zarahn E, Alsop DC (2002) Experimental design and the relative sensitivity of BOLD and perfusion fMRI. Neuroimage 15: 488–500

Alsop DC, Detre JA, Grossman M (2000) Assessment of cerebral blood flow in Alzheimer's disease by spin-labeled magnetic resonance imaging. Ann Neurol 47: 93–100

Blamire AM, Ogawa S, Ugurbil K, Rothman D, McCarthy G, Ellermann JM, Hyder F, Rattner Z, Shulman RG (1992) Dynamic mapping of the human visual cortex by high-speed magnetic resonance imaging. Proc Natl Acad Sci USA 89: 11069–11073

Boynton GM, Engel SA, Glover GH, Heeger DJ (1996) Linear systems analysis of functional magnetic resonance imaging in human V1. J Neurosci 16: 4207–4221

Buxton RB, Frank LR, Wong EC, Siewert B, Warach S, Edelman RR (1998) A general kinetic model for quantitative perfusion imaging with arterial spin labeling. Magn Reson Med 40: 383–396

Buxton RB, Uludag K, Dubowitz DJ, Liu TT (2004) Modeling the hemodynamic response to brain activation. Neuroimage 23 [Suppl 1]: S220–S233

Calamante F, Thomas DL, Pell GS, Wiersma J, Turner R (1999) Measuring cerebral blood flow using magnetic resonance imaging techniques. J Cereb Blood Flow Metab 19: 701–735

Chen W, Ugurbil K (1999) High spatial resolution functional magnetic resonance imaging at very-high-magnetic field. Top Magn Reson Imaging 10: 63–78

Detre JA, Alsop DC (1999) Perfusion magnetic resonance imaging with continuous arterial spin labeling: methods and clinical applications in the central nervous system. Eur J Radiol 30: 115–124

Detre JA, Leigh JS, Williams DS, Koretsky AP (1992) Perfusion imaging. Magn Reson Med 23: 37–45

Detre JA, Wang J (2002) Technical aspects and utility of fMRI using BOLD and ASL. Clin Neurophysiol 113: 621–634

DeYoe EA, Bandettini P, Neitz J, Miller D, Winans P (1994) Functional magnetic resonance imaging (FMRI) of the human brain. J Neurosci Methods 54: 171–187

Di Salle F, Formisano E, Linden DE, Goebel R, Bonavita S, Pepino A, Smaltino F, Tedeschi G (1999) Exploring brain function with magnetic resonance imaging. Eur J Radiol 30: 84–94

Dougherty RF, Koch VM, Brewer AA, Fischer B, Modersitzki J, Wandell BA (2003) Visual field representations and locations of visual areas V1/2/3 in human visual cortex. J Vis 3: 586–598

Feng CM, Narayana S, Lancaster JL, Jerabek PA, Arnow TL, Zhu F, Tan LH, Fox PT, Gao JH (2004) CBF changes during brain activation: fMRI vs. PET. Neuroimage 22: 443–446

Fox PT, Raichle ME (1984) Stimulus rate dependence of regional cerebral blood flow in human striate cortex, demonstrated by positron emission tomography. J Neurophysiol 51: 1109–1120

Fox PT, Raichle ME (1985) Stimulus rate determines regional brain blood flow in striate cortex. Ann Neurol 17: 303–305

Garraux G, Hallett M, Talagala SL (2005) CASL fMRI of subcortico-cortical perfusion changes during memory-guided finger sequences. Neuroimage 25: 122–132

Gonzalez-At JB, Alsop DC, Detre JA (2000) Cerebral perfusion and arterial transit time changes during task activation determined with continuous arterial spin labeling. Magn Reson Med 43: 739–746

Hansen KA, David SV, Gallant JL (2004) Parametric reverse correlation reveals spatial linearity of retinotopic human V1 BOLD response. Neuroimage 23: 233–241

Hasnain MK, Fox PT, Woldorff MG (1998) Intersubject variability of functional areas in the human visual cortex. Hum Brain Mapp 6: 301–315

Hoge RD, Atkinson J, Gill B, Crelier GR, Marrett S, Pike GB (1999) Stimulus-dependent BOLD and perfusion dynamics in human V1. Neuroimage 9: 573–585

Kemeny S, Ye FQ, Birn R, Braun AR (2004) Comparison of continuous overt speech fMRI using BOLD and arterial spin labeling. Hum Brain Mapp 24: 173–183

Kwong KK, Belliveau JW, Chesler DA, Goldberg IE, Weisskoff RM, Poncelet BP, Kennedy DN, Hoppel BE, Cohen MS, Turner R (1992) Dynamic magnetic resonance imaging of human brain activity during primary sensory stimulation. Proc Natl Acad Sci USA 89: 5675–5679

Lai S, Hopkins AL, Haacke EM, Li D, Wasserman BA, Buckley P, Friedman L, Meltzer H, Hedera P, Friedland R (1993) Identification of vascular structures as a major source of signal contrast in high resolution 2D and 3D functional activation imaging of the motor cortex at 1.5 T: preliminary results. Magn Reson Med 30: 387–392

Lehmann C, Mueller T, Federspiel A, Hubl D, Schroth G, Huber O, Strik W, Dierks T (2004) Dissociation between overt and unconscious face processing in fusiform face area. Neuroimage 21: 75–83

Luh WM, Wong EC, Bandettini PA, Hyde JS (1999) QUIPSS II with thin-slice TI1 periodic saturation: a method for improving accuracy of quantitative perfusion imaging using pulsed arterial spin labeling. Magn Reson Med 41: 1246–1254

Mandeville JB, Marota JJ, Ayata C, Zaharchuk G, Moskowitz MA, Rosen BR, Weisskoff RM (1999) Evidence of a cerebrovascular postarteriole windkessel with delayed compliance. J Cereb Blood Flow Metab 19: 679–689

Miller KL, Luh WM, Liu TT, Martinez A, Obata T, Wong EC, Frank LR, Buxton RB (2001) Nonlinear temporal dynamics of the cerebral blood flow response. Hum Brain Mapp 13: 1–12

Obata T, Liu TT, Miller KL, Luh WM, Wong EC, Frank LR, Buxton RB (2004) Discrepancies between BOLD and flow dynamics in primary and supplementary motor areas: application of the balloon model to the interpretation of BOLD transients. Neuroimage 21: 144–153

Ogawa S, Menon RS, Tank DW, Kim SG, Merkle H, Ellermann JM, Ugurbil K (1993) Functional brain mapping by blood oxygenation level-dependent contrast magnetic resonance imaging. A comparison of signal characteristics with a biophysical model. Biophys J 64: 803–812

Oldfield RC (1971) The assessment and analysis of handedness: the Edinburgh inventory. Neuropsychologia 9: 97–113

Roberts DA, Detre JA, Bolinger L, Insko EK, Leigh JS Jr (1994) Quantitative magnetic resonance imaging of human brain perfusion at 1.5 T using steady-state inversion of arterial water. Proc Natl Acad Sci USA 91: 33–37

Rombouts SA, Barkhof F, Hoogenraad FG, Sprenger M, Scheltens P (1998) Within-subject reproducibility of visual activation patterns with functional magnetic resonance imaging using multislice echo planar imaging. Magn Reson Imaging 16: 105–113

Silva AC, Lee SP, Iadecola C, Kim SG (2000) Early temporal characteristics of cerebral blood flow and deoxyhemoglobin changes during somatosensory stimulation. J Cereb Blood Flow Metab 20: 201–206

Silva AC, Lee SP, Yang G, Iadecola C, Kim SG (1999) Simultaneous blood oxygenation level-dependent and cerebral blood flow functional magnetic resonance imaging during forepaw stimulation in the rat. J Cereb Blood Flow Metab 19: 871–879

Talagala SL, Ye FQ, Ledden PJ, Chesnick S (2004) Whole-brain 3D perfusion MRI at 3.0 T using CASL with a separate labeling coil. Magn Reson Med 52: 131–140

Talairach J, Tournoux P (1988) Co-planar stereotaxic atlas of the human brain: 3-dimensional proportional system: an approach to cerebral imaging. Thieme, Stuttgart New York

Wang J, Aguirre GK, Kimberg DY, Detre JA (2003a) Empirical analyses of null-hypothesis perfusion FMRI data at 1.5 and 4 T. Neuroimage 19: 1449–1462

Wang J, Aguirre GK, Kimberg DY, Roc AC, Li L, Detre JA (2003b) Arterial spin labeling perfusion fMRI with very low task frequency. Magn Reson Med 49: 796–802

Wang J, Licht DJ, Jahng GH, Liu CS, Rubin JT, Haselgrove J, Zimmerman RA, Detre JA (2003c)

Pediatric perfusion imaging using pulsed arterial spin labeling. J Magn Reson Imaging 18: 404–413
Wang J, Wang Z, Aguirre GK, Detre JA (2005) To smooth or not to smooth? ROC analysis of perfusion fMRI data. Magn Reson Imaging 23: 75–81
Wong EC, Buxton RB, Frank LR (1997) Implementation of quantitative perfusion imaging techniques for functional brain mapping using pulsed arterial spin labeling. NMR Biomed 10: 237–249
Wong EC, Buxton RB, Frank LR (1998) Quantitative imaging of perfusion using a single subtraction (QUIPSS and QUIPSS II). Magn Reson Med 39: 702–708
Wong EC, Buxton RB, Frank LR (1999) Quantitative perfusion imaging using arterial spin labeling. Neuroimaging Clin North Am 9: 333–342
Yang Y, Engelien W, Pan H, Xu S, Silbersweig DA, Stern E (2000) A CBF-based event-related brain activation paradigm: characterization of impulse-response function and comparison to BOLD. Neuroimage 12: 287–297
Yang Y, Gu H, Stein EA (2004) Simultaneous MRI acquisition of blood volume, blood flow, and blood oxygenation information during brain activation. Magn Reson Med 52: 1407–1417
Zhu XH, Kim SG, Andersen P, Ogawa S, Ugurbil K, Chen W (1998) Simultaneous oxygenation and perfusion imaging study of functional activity in primary visual cortex at different visual stimulation frequency: quantitative correlation between BOLD and CBF changes. Magn Reson Med 40: 703–711

Author's address: A. Federspiel, PhD, Department of Psychiatric Neurophysiology, University Hospital of Clinical Psychiatry, Bollingenstrasse 111, 3000 Bern 60, Switzerland, e-mail: federspiel@puk.unibe.ch